IC/92/429

INTERNATIONAL CENTRE FOR
THEORETICAL PHYSICS

STATUS OF THE MSW-SOLUTION OF THE SOLAR NEUTRINO PROBLEM

Alexei Yu. Smirnov

INTERNATIONAL ATOMIC ENERGY AGENCY

UNITED NATIONS EDUCATIONAL, SCIENTIFIC AND CULTURAL ORGANIZATION

MIRAMARE-TRIESTE

IC/92/429

International Atomic Energy Agency

and

United Nations Educational Scientific and Cultural Organization

INTERNATIONAL CENTRE FOR THEORETICAL PHYSICS

STATUS OF THE MSW-SOLUTION OF THE SOLAR NEUTRINO PROBLEM *

Alexei Yu. Smirnov **

International Centre for Theoretical Physics, Trieste, Italy.

MIRAMARE – TRIESTE

December 1992

* Talk given at the International Symposium on Neutrino Astrophysics, Takayama/Kamioka 19–22 October 1992.

** On leave of absence from: Institute for Nuclear Research, Russian Academy of Sciences, 117312 Moscow, Russia.
E-mail: smirnov@itsistp.bitnet

ABSTRACT

Status of the resonant flavor conversion is formulated in view of latest solar neutrino data. We discuss different methods of determination of neutrino parameters. The effects of third neutrino admixture as well as possible nonvacuum mixing are considered.

1. Introduction

There are two aspects of the application of the resonant flavor conversion (MSW-effect) [1] to solar neutrinos: (1) the conversion can explain the deficit of ν_e - signal [2 - 5], (2) properties of solar neutrino fluxes give the information on neutrino masses (Δm^2) and mixing ($\sin^2 2\theta$). Consequently the output of this study will be

- either *determination* of the neutrino parameters, Δm^2, $\sin^2 2\theta$, if the $\nu_\odot$-problem exists and the MSW effect is its solution,

- or *exclusion* of definite domain on $\Delta m^2 - \sin^2 2\theta$ - plot if the conversion does nothing with solar neutrinos (i.e. there is no $\nu_\odot$- problem or some other mechanism is responsible for $\nu_\odot$-deficit).

At present we are in the middle of the way: no final conclusion can be made on the existence of the resonance conversion of solar neutrinos. The results concerning with determination of the neutrino parameters *must be considered as tentative* ones. The sense of present analyses is to give some hits to future experiments and to elaborate the methods of treating the data which will be used in future determination/exclusion work.

2. Solar neutrino data

The ratios of the observed signals to the central values of signals predicted by the Standard Solar Model (SSM) [6] (see also [7]) equal:

$$R_{Ar} = 0.28 \pm 0.03, \quad R_{\nu e} = 0.49 \pm 0.08, \quad R_{Ge} = 0.63 \pm 0.16 \qquad (1)$$

for Cl - Ar [2], Kamiokande II + III [3] and Gallium experiment [4] correspondently (Gallex data are used here).

There are two important observations:

1) Cl - Ar -signal is suppressed more stronger than the Kamiokande one:

$$\frac{R_{Ar}}{R_{\nu e}} = 0.58 \pm 0.12. \tag{2}$$

Moreover, the contribution of the boron neutrino flux measured by the Kamiokande to the Ar-production rate equals $Q^B_{Ar} = (3.1 \pm 0.5) SNU$. This is even bigger than total signal measured by Cl - Ar detector in series after 1986 [2]. Consequently, the berillium neutrino flux which also contributes to Ar-production rate should be strongly suppressed.

2). Gallium experiment shows the weakest suppression of signal. Moreover, the central value of GALLEX experiment is a little bit higher than the contribution of pp-neutrino flux to germanium production rate: $Q^{pp}_{Ge} \approx 70 SNU$.

The observations indicate on the energy dependence of flux suppression:

- pp-neutrinos (low energy part of spectrum) are unsuppressed or weakly suppressed;
- berillium neutrino flux (middle energies) is strongly suppressed;
- boron neutrinos (high energies) have moderate ($\approx 1/2$) suppression.

This, in particular, disfavour the astrophysical solution (for details see [8]).

3. Islands on the $\Delta m^2 - \sin^2 2\theta$ plot

The suppression of the ν_e-flux due to the MSW-effect depends on neutrino energy, as well as on Δm^2 and $\sin^2 2\theta$: $P = P(E, \Delta m^2, \sin^2 2\theta)$. The regions on $\Delta m^2 - \sin^2 2\theta$-plot can be found in which one can reconcile the observed signals with the SSM predictions. Moreover, both experimental errors and the astrophysical uncertainties in predicted signals should be taken into account simultaneously. For this several approaches are used: the intersections of allowed regions, χ^2-method, Monte-Carlo simulation.

The intersection of allowed regions [9 - 12] is the most simple and straightforward method. The procedure is the following: one (1) fixes the astrophysical parameters and thus the predicted fluxes, (2) finds for each experiment the allowed region of $\Delta m^2 - \sin^2 2\theta$ which correspond to definite level of experimental errors (1σ, 2σ etc.), (3) finds the intersection of these allowed regions, (4) chooses another set of astrophysical parameters (neutrino fluxes) from some allowed domain as input and finds new intersection regions. Then the overlap of all such regions gives the idea on the astrophysical uncertainties.

Obviously, the method does not allow to prescribe definite confidence level for the obtained regions.

The intersection regions allowed by 2σ data from the Cl - Ar, Kamiokande and GALLEX experiments are shown in Fig.1a [12]. The predictions of SSM [6] have been used. Following comments are in order.

1). There are two intersection regions corresponding to two types of solutions. The region of *small mixing* solutions can be parametrized for $T_c = T_c^{SSM}$ as

$$\Delta m^2 = \frac{(4.7 \pm 1.6)\cdot 10^{-8}}{\sin^2 2\theta} eV^2, \quad \sin^2 2\theta = (0.4 - 1.3)\cdot 10^{-2}. \tag{3}$$

The region of *big mixings* has two parts - the upper one

$$\Delta m^2 = (0.35 - 9)\cdot 10^{-5} eV^2, \quad \sin^2 2\theta = 0.4 - 0.8, \tag{4}$$

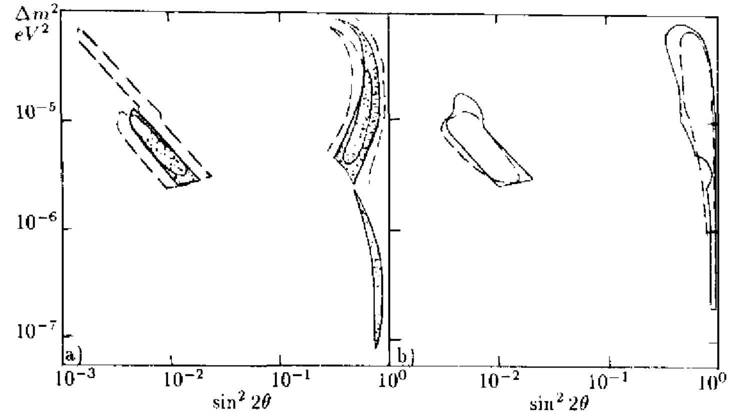

Figure 1. Regions of the neutrino parameters defined from solar neutrino data. a). The intersection of 2σ-allowed regions for $T_c = T_c^{SSM}$ (solid lines), $T_c = 1.012 T_c^{SSM}$ and $T_c = 0.988 T_c^{SSM}$ (dashed lines). Also the domain defined by χ^2 for fixed astrophysical parameters is shown [13]. b). χ^2 method results with astrophysical uncertainties taken into account [14] (dashed lines), Monte Carlo simulations [16] (solid lines).

and the bottom one

$$\Delta m^2 = (0.08 - 2)\cdot 10^{-6} eV^2, \quad \sin^2 2\theta = 0.5 - 0.9. \tag{5}$$

These two parts are separated by the region of strong matter effect (day - night, seasonal) which is excluded by Kamiokande data at 1.5σ level.

2). At 1.5σ-experimental level the bottom part of large mixing region disappears.

3). The calculations by different authors are in qualitative agreement and the difference is related to ΔR_{Ar} the value of error of the Cl - Ar result used, or to the Earth matter effect (in some papers it is ignored or treated incorrectly), or to Kamiokande data: some authors used the data from Kamiokande-II only.

4). As follows from fig.1a GALLEX excludes essential part of the "nonadiabatic region" and lepton mixing equal to Cabibbo mixing is disfavoured.

χ^2-fit of the data [13,14]. One can perform a combined analysis of the data by defining the minimum of

$$\chi^2 = \sum_{i=Ar,\nu e,Ge} [R_i^{obs} - R_i(\Delta m^2, \theta)]^2/\sigma_i^2 \tag{6}$$

Here R_i^{obs} and R_i are the observed and the predicted suppression factors correspondently. The astrophysical parameters are considered to be fixed. Then $\Delta m^2 - \sin^2 2\theta$ region allowed at 90% CL is found from the condition

$$\chi^2(\Delta m^2, \theta) = \chi^2_{min} + 4.6$$

(fig.1a). Note that only two regions survive. The astrophysical uncertainties can be also included in χ^2 analysis [14] (fig.1b).

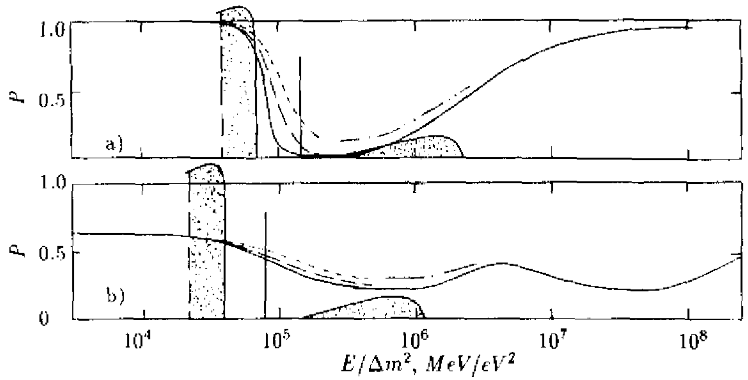

Figure 2. *The dependence of the suppression factor on energy: a). small mixing solution, b). big mixing solution. Respective position of the solar neutrino spectrum is also shown.*

Let us comment on properties of the solutions. In case of *small mixing* the suppression pit is thin (fig.2a). The solution has the following features:
- pp-neutrino flux is outside the pit and thus practically unsuppressed;
- Be-neutrino flux is strongly or moderately suppressed (depending on Δm^2): $P_{Be} = 10^{-3} - 0.6$;
- boron neutrinos are moderately suppressed: $P \approx 1/2$;
(*Note that these features fit well the experimental indications.*)
- the energy spectrum of boron neutrinos has nonadiabatic distortion: $P \propto exp(-E_o/E)$;
- the Earth matter effects are very small.

In case of *large mixing solution* (Fig.2b) the suppression pit is big. Outside its left edge the suppression stipulated by vacuum oscillations, $P \approx 1 - \sin^2 2\theta/2$, is not small. The bump in the middle part of the pit ($E \approx 10^6 - 10^7 MeV/eV^2$) is due to the effect of ν_e-regeneration in the Earth.

The upper part of the region (Fig.1a) corresponds to situation when boron neutrino spectrum lies at energies smaller than the bump energy. In this case
- pp-neutrinos are outside the pit undergoing the vacuum oscillations $P \approx 0.6 - 0.8$;
- Be-neutrinos are on the left edge of pit and $R_{Be} \approx 0.20 - 0.65$;
- boron neutrinos are on the bottom of the pit and their energy spectrum is practically undistorted. The distortion may be induced by the Earth matter effect when high energy part of spectrum falls in the regeneration peak;
- high energy part of ν_B-specrum may have day-night and seasonal variations.

For bottom part of large mixing region (fig.1a) one has the following:
- pp-neutrinos are on the bottom of the pit and thus their flux is appreciably suppressed $P = 0.4 - 0.6$ (for this reason the solution marginally agrees with the data),
- boron neutrino spectrum is in the bottom or on the nonadiabatic edge of the pit, and thus can be distorted;
- the Earth matter effect is expected for Be- or pp- neutrinos.

Future experiments with big statistics will be able to distinguish the solutions. The crucial points are: the measurements of signals with good precision, search for a distortion of the boron neutrino spectrum. The detection of Be-neutrino flux as well as search for the time variations of signals are of great importance.

4. Astrophysical uncertainties

Changes of the astrophysical parameters result in correlated changes of the neutrino fluxes and, consequently, the signals. Moreover, the signals from different experiments depend on the same fluxes although with different weights. There are several ways to include the astrophysical uncertainties in the determination of $\Delta m^2 - \sin^2 2\theta$ taking into account the correlations. The simplest way is just to find the intersection regions for different SSM. More sofisticated possibilities are based on "1000SSM-method" by Bahcall and Ulrich [6,10]. The idea is the following. Main uncertainties in neutrino fluxes are related to five parameters: the relative concentration of heavy elements, Z/X, and four cross sections σ_{11} (p + p), σ_{33} ($^3He +^3 He$), σ_{34} ($^3He +^4 He$), σ_{17} ($p +^7 Be$). The parameters are used as the input for construction *of the consistent SSM which satisfies the observations. The model gives as the output* both solar characteristics (such as central temperature, T_c, the density profile etc.) and the neutrino fluxes. Suggesting the normal distribution for mentioned parameters 1000 Monte Carlo simulations have been performed i.e. 1000SSM and therefore 1000 sets of (T_c, F_B, F_{Be} ...) have been found. This in turns enables to construct the *distributions of the output parameters. In particular, it has been found for* T_c:

$$\frac{\Delta T_c}{T_c} = 1.2\% \tag{7}$$

at 2σ level. The "1000SSM" shows strong correlation of central temperature and the neutrino fluxes. The correlations for the most important fluxes can be approximated by [6]:

$$F_B \propto T_c^{18}, \quad F_{Be} \propto T_c^8, \quad F_{pp} \propto T_c^{-1.2}. \tag{8}$$

One can fix the highest, T_c^h, and the lowest, T_c^l, central temperatures which correspond, let say, to 2σ deviation from central value. According to (7): $T_c^l = 0.988T_c$ and $T_c^h = 1.012T_c$. Then using the dependences (8) one can find the neutrino fluxes and the intersection regions for T_c^l and T_c^h (fig.1a). Note that variations of T_c result in a shift of the allowed region but not in appreciable change of its size. With increasing temperature a small allowed region appears for smaller mixing angles. The reason is that for big T_c the respective contribution of Be-neutrinos to Ar-production rate diminishes: $F_B/F_{Be} \propto T^{10}$ thus immitating a situation of strong F_{Be} suppression. This improves an agreement between Cl - Ar and Kamiokande data.

The results of χ^2-method [14] are shown in fig.1b.. It is possible to consider T_c as a fit parameter in χ^2-method, So that $\chi^2 = \chi^2(\Delta m^2, \sin^2 2\theta, T_c)$. It was found [14] by using the dependences (8) that the most probable values of parameters are $T_c = 1.03T_c^{SSM}$, $\Delta m^2 = 8.9 \cdot 10^{-6} eV^2$, $\sin^2 2\theta = 7.7 \cdot 10^{-3}$. Note that T_c turns out to be outside the 2σ interval allowed by SSM. With only three measurements this method has no big sense: to fit them three parameters are used.

More consistent method [16] (see also [17]) is to use immediately the distributions of (T_c, F_B, F_{Be} etc.) obtained by 1000SSM simulations, rather than the approximation (8). For each pair of values of the parameters ($\Delta m^2, \theta$) 1000SSM simulations are performed. This gives 1000 sets of ($R_{\nu e}$, R_{Ar}). Then 95% CL (2σ) allowed region on ($\Delta m^2 - \sin^2 2\theta$) plot can be found by the following criteria. Given ($\Delta m^2, \theta$) point is inside the 2σ domain if for this point more than 50 (i.e. 5%) models from 1000 ones give the ($R_{\nu e}, R_{Ar}$) values in 2σ domain for $R_{\nu e}$- , R_{Ar}- measurements.

Obviously, the method can be generalized for three measurements i.e. including also R_{Ge}.

As it follows from fig.1a,b the results of different approaches are in reasonable agreement.

5. Three neutrino mixing case

In three neutrino case there is a variety of possibilities which differ by values of neutrino parameters and by dependences of the suppression factors on the neutrino energy. These possibilities can be classified by using unique $\Delta m^2 - \sin^2 2\theta$-plot [18]. Indeed it can be shown that as far as we deal with conversion of the electron neutrinos the three neutrino system can be described by two sets of vacuum parameters: $N_{12} \equiv (\Delta m_{12}^2, \sin^2 2\theta_{12})$ and $N_{13} \equiv (\Delta m_{13}^2, \sin^2 2\theta_{13})$ which are defined in the following way. In vacuum the ν_e-state can be presented as

$$\nu_e = \cos\theta_{13} \cdot \tilde{\nu} + \sin\theta_{13} \cdot \nu_3, \tag{9}$$

where

$$\tilde{\nu} = \cos\theta_{12} \cdot \nu_1 + \sin\theta_{12} \cdot \nu_2. \tag{10}$$

Here Δm_{12}^2 and Δm_{13}^2 are the mass squared differences of ν_1, ν_2 and ν_1, ν_3 neutrinos correspondently.

Thus with respect to ν_e conversion the 3ν system is fixed by two points (N_{12} and N_{13}) on $\Delta m^2 - \sin^2 2\theta$ plot. Moreover, a position of these points with respect to "the resonance triangle" for 2ν-conversion plays crucial role (see fig.3). If one of the points N_{1i} is far away from the resonance triangle then corresponding mixing does not participate in dynamics of conversion and the task is reduced to 2ν-task. Now to solve the $\nu_{\odot}$ problem second point should be in resonance triangle, moreover,

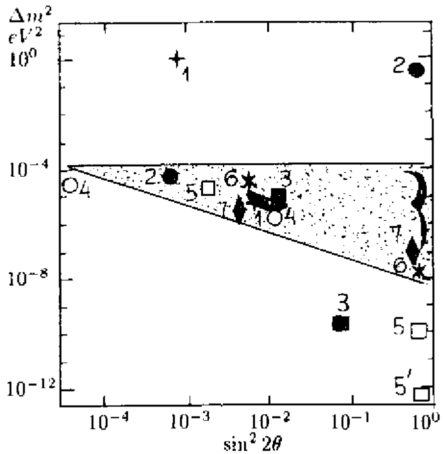

Figure 3. Positions of neutrino parameters points in case for three neutrino mixing.

ISOSNU lines for this point will coincide with corresponding ISOSNU lines for 2ν-conversion. The exclusion from this rule is the case of big angle θ_{13} (see below). Let us comment on the most interesting special cases.

1. *The mass m_3 (N_{13}) is far above the resonance triangle.* Then N_2 should be in the resonance triangle. This scenario follows naturally from the see-saw mechanism with majorana mass term for right component of the order of $(0.01 - 1) \cdot 10^{12}$ GeV. If $m_3 \geq 1eV$ then ν_3 can respect for the cosmological problems. At $m_3 \approx 0.1eV$ the oscillations $\nu_\mu - \nu_\tau$ may explain the atmospheric neutrino deficit. Moreover, the oscillations of neutrinos with $\Delta m^2 \approx m_3^2 \geq 10^{-2}eV^2$ can be observed in new accelerator experiments.

Now if $m_3^2 \gg m_c^2 \equiv 10^{-4}eV^2$ (m_c corresponds to resonance for neutrinos with energy 10 MeV in the center of the Sun) then mixing of ν_3 does not practically differ from vacuum mixing durning the propagation:

$$\sin^2 2\theta_{13}^m \approx \frac{\sin^2 2\theta_{13}}{1 - 2\cos 2\theta_{13} \cdot l_\nu / l_o}, \tag{11}$$

where $l_\nu/l_o < m_c^2/m_3^2 \ll 1$. Since the propagation of ν_{3m} is far from resonant one, the adiabaticity condition is well fulfilled [1]. Therefore the admixture of ν_{3m} eigenstate in $\nu(t)$ is constant being fixed in the production point: $\theta_{13}^m = \theta_{13}^{m,o}$. Then the only process which ν_{3m} participate in is the oscillations and since the corresponding Δm^2 is big these oscillations will be averaged out. Thus during the propagation $\tilde{\nu}$ will undergo the resonant conversion into its orthogonal state $\nu' = \cos\theta_{12}\nu_2 - \sin\theta_{12}\nu_1$ and the splitting between the energies of $\tilde{\nu}$, ν' and ν_{3m} will induce the oscillations with small oscillation length. The ν_e survival probability can be written immediately:

$$P = \cos^2\theta_{13}^{m,o} \cdot \cos^2\theta_{13} \cdot P_2 + \sin^2\theta_{13}^{m,o} \cdot \sin^2\theta_{13}. \tag{12}$$

Here P_2 is the survival probability with respect to two neutrino conversion $\tilde{\nu} \to \nu'$. If θ_{13} is small enough (see conf. 1-1) then $P \approx P_2$ and the task is completely reduced to 2ν-case.

The appreciable influence of third neutrino on ν_e flux appears when $e-\tau$ mixing is big [19] (conf. 2-2, although such a situation seems not to be natural). Neglecting small matter corrections to $\sin\theta_{13}^2$ one has

$$P = \cos^4\theta_{13} \cdot P_2 + \sin^4\theta_{13}. \tag{13}$$

For $P_2(\Delta m_{12}^2, \sin^2 2\theta_{12})$ the usual 2ν-suppression pit can be used. At $\sin^2 2\theta_{13} > 0.5$ new region in the plot for 2ν becomes allowed: $\sin^2 2\theta_{12} \approx (1-3) \cdot 10^{-3}$. For such values of θ_{12} the mutual position of the spectrum and the suppression pit is shown in fig.4a. Now both pp-neutrino and Be-neutrino fluxes are moderately suppressed by factor of $P = (1 - \sin^2 2\theta_{13}/2)$ which corresponds to vacuum oscillation $\nu_e \to \nu_\tau$. The distortion of boron neutrino spectrum may be nonadiabatic or even more complicated with strongest suppression in the middle energy part.

2. *N_1 (or N_2) is below the diagonal edge of the resonance triangle.* There are several phenomenologically different possibilities (see fig.4).

a). In 3-3 case N_{13} is in the resonance triangle, whereas N_{12} is below it, moreover, θ_{12} is small. Consequently, before resonance region the $\tilde{\nu} \to \nu'$ conversion is suppressed by matter effect; in the resonance region there is no transformation due to strong adiabaticity violation (resonance region is too thin); after resonance vacuum

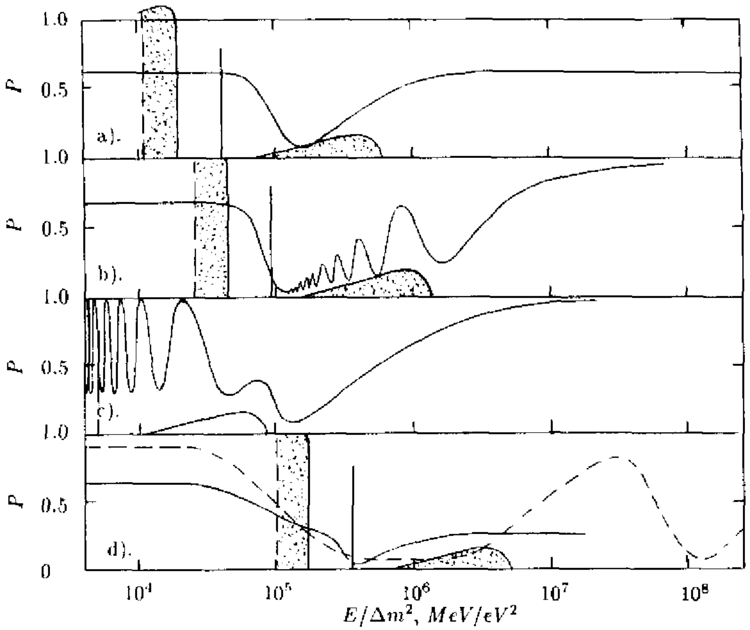

Figure 4. The dependence of the suppression factors in 3ν case on energy for different sets of neutrino parameters (see fig.3): a) 2-2, b). 5-5, c). 5-5', d). 6-6, e). 7-7.

oscillations can be neglected since the angle θ_{12} is small. So, the task is again reduced to two neutrino case: ν_e converts into ν_τ via θ_{13} mixing and $\tilde{\nu}$ can be considered as the eigenstate.

b). The same situation is in 4-4 case, where N_{12} is in the triangle, N_{13} lies below it and θ_{13} is small. Similar consideration shows that ν_3 does not participate *practically in the transitions and ν_e-flux is determined by the conversion $\nu_e \to \nu_\mu$* (stipulated by 2ν-conversion $\tilde{\nu} \to \nu'$).

c). Let N_{12} is below the triangle but θ_{12} is big (5-5 case). Now the oscillations $\tilde{\nu} \to \nu'$ are suppressed by matter and inside the Sun the resonant conversion $\nu_e \to \nu_\tau$ takes place due to N_{13} mixing ($\tilde{\nu} - \nu_3$). But at $\Delta m_{12}^2 > 10^{-11} eV^2$ the vacuum oscillations $\tilde{\nu} - \nu'$ become essential on the way from the surface of the Sun to the Earth. These oscillations modify the edges of matter suppression pit (the bottom of the pit corresponds to pure ν_3 state and the latter obviously does not oscillate in vacuum). Then for small θ_{13} the total suppression pit is defined approximately by the product $P \approx P_\rho \cdot P_v$, where P_ρ and P_v are the survival probabilities for ν_e in matter and in vacuum (on the way from the Sun to the Earth). Variety of new forms of the suppression pits appear depending on ratio r = $\Delta m_{12}^2/\Delta m_{13}^2$. If r $\gg 10^{-6}$, then vacuum oscillation pit lies at bigger energies than resonant conversion pit, at $r \ll 10^{-6}$ - vice versa (see fig.4b,c). Now new regions for N_{13} become possible. In particular, for

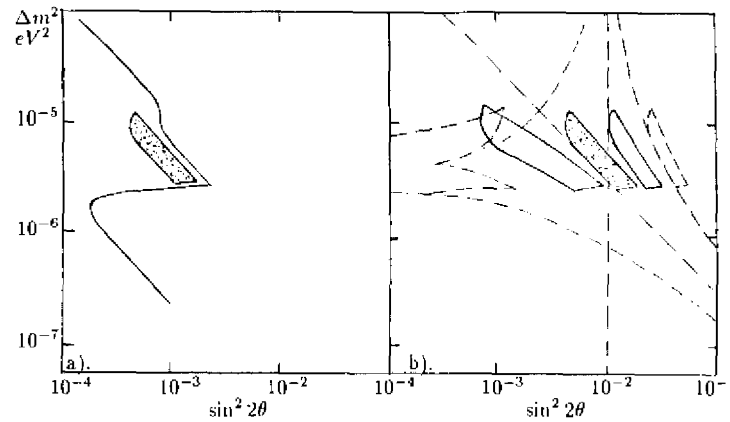

Figure 5. Modification of the allowed small mixing region due to a). effect of third neutrino, b). additional nonvacuum mixing: ϵ = 0.02 (solid lines), ϵ = 0.05 (dashed lines).

the configuration of fig.4b the values of $\sin^2 2\theta_{13}$ upto 10^{-3} are not excluded.

3. *Both points, N_{12} and N_{13}, are in the resonance triangle.* The influence of one resonance on another one may take place. But again if there is a strong mass hierarchy and the mixing is small, then two resonance conversions, $\nu_e - \nu_\mu$ and $\nu_e - \nu_\tau$, occur in different spatial regions, and crossing of resonances is *dynamically* independent. In this case a factorization of total survival probability takes place [17]: $P \approx P_{12} \cdot P_{13} + O(\sin^2\theta_{13})$, where P_{12} and P_{13} are the 2ν-survival probabilities. Correspondently the total suppression pit is some superposition of 2ν-suppression pits (fig.4d). Note that the configurations of Fig.4d, when pp-neutrinos spectrum is in the second pit, is disfavoured by GALLEX data. But the another configuration of Fig.4d opens an interesting possibility to have strong suppression of the Be-neutrino line and undistorted boron neutrino spectrum.

6. MSW effect and non-vacuum mixing.

Flavor mixing considered above is induced by the vacuum, i.e. the nondiagonal mass terms. Besides this other contributions to flavor mixing can exist. In particular, the effective mixing can be induced by the scattering of neutrinos on real particles of matter. The interesting possibility is the neutrino scattering via exchange of *charged scalar particle*. The scalar with charge 1 may have the flavor off diagonal couplings: $h\bar{e}_R\nu_{\tau L}\phi$ [20]. Or it may have fractional charge being the superpartner of quark: $\tilde{b}^{1/3}$ [21,22]. In supersymmetric theories with with R-parity violation such a boson may have the couplings $h_e\bar{\nu}_{eL}d_R\tilde{b} + h_\tau\bar{\nu}_\tau d_R\tilde{b}$ + h.c.. The latter will generate via $\tilde{b}$ exchange the effective $\nu_e - \nu_\tau$ transition in scattering on d-quarks. Now (in contrast with standard case) the matter contribution to the evolution matrix is nondiagonal:

$$H_\rho = \sqrt{2}G_F\rho \cdot \begin{pmatrix} 1+\epsilon' & \epsilon \\ \epsilon & 0 \end{pmatrix}, \tag{14}$$

where ϵ' and ϵ parameters describing new interactions. At $\epsilon > 10^{-2}$ their contribution can essentialy change the allowed region of neutrino parameters. In particular, the resonant conversion can take place even at zero vacuum mixing.

If new contributions comes from scattering on electrons only, or if the chemical composition is approximately the same on the way of neutrinos, then ϵ, ϵ' are constants. In this case it is instructive to make the rotation of flavor states $\nu_f = S(\alpha) \cdot \nu'_f$, where α is defined by

$$\tan 2\alpha = \frac{2\epsilon}{1+\epsilon'}$$

For ν'_f the matter effect is diagonal and the evolution matrix is reduced to the usual one by redefinition

$$\theta \to \theta + \alpha$$

At small α the survival probability for the original flavor states is $P_\epsilon(\theta) = P'(\Delta m^2, \theta - \alpha)$ where P' is the survival probability for ν'_e. The allowed region of neutrino parameters can be found by rescalling of θ variable. New contribution modifies the ISOSNU contours and the intersection regions at $\theta \leq \alpha$. The critical point is $\theta = \alpha$ If θ and α are of the same sign then the points placed at $\theta' = \alpha$ for "standard conversion" are shifted to $\theta \to 0$, and at $\theta' \to 0$ the points approach the vertical line $\theta = \alpha$. If θ and α are of the opposite sign then all points are at $\theta' < \alpha$, and they approach $\theta = \alpha$ when $\theta \to 0$ (see Fig.5). For more details see [23,24]. As follows from Fig.5 the allowed regions may be essentially modified and shifted.

7. Conclusions

1. Resonance flavor conversion is flexible mechanism for solution of the $\nu_\odot$-problem. It can fit all existing data and will fit the data which appear in future. Moreover, the conversion can saturate the model independent limits (which follow just from the consistency of experimental data). A variety of energy spectrum distortions can be obtained.

2. Present data pick up rather small regions of neutrino parameters. Small mixing region is in favour, but many other regions can not be excluded.

3. The astrophysical uncertainties enlarge the allowed regions. Several methods are suggested to treat these uncertainties. The most consistent method of determination of the neutrino parameters implies the inclusion of *both the astrophysical parameters and the values of measured signals* into the Monte Carlo games.

4. Third neutrino also enlarges allowed regions. But in most interesting cases the effect of third neutrino is small and 3ν-task is reduced to 2ν-task. Some configurations with *three neutrinos* are excluded already. *In the same time* there are the nontrivial configurations which give new types of neutrino spectrum distortion. Thus clear signature of appreciable admixture of third neutrino appears.

5. New contributions to neutrino mixing which follow from physics beyond the standard model can essentially modify the allowed regions of parameters.

References

1. S.P.Mikheyev and A.Yu.Smirnov, Sov.J.Nucl.Phys. 42 (1986) 913, Prog. in Part. and Nucl.Phys., 23 (1989) 41;
   L.Wolfenstein, Phys.Rev. D17 (1978) 2369, D20 (1979) 2634;
   T.K.Kuo and J. Pantaleone, Rev.Mod.Phys., 61 (1989) 937.
2. R.Davis, these Proceedings.
3. K.S.Hirata et. al., Phys.Rev.Lett., 66 (1991) 9; Phys.Rev., D44 (1991) 2241; these Proceedings.
4. A.I.Abazov et al., Phys.Rev.Lett., 67 (1991) 3332;
   G.T.Zatsepin, these Proceedings.
5. P.Anselmann et. al., Phys.Lett.,B285 (1992) 376.
6. J.N.Bahcall and R.K.Ulrich, Rev.Mod.Phys., 60 (1988) 297; J.N.Bahcall and M.H.Pinsonneault, Rev.Mod.Phys., 64 (1992) 885.
7. S.Turck-Chieze et al., Astroph. J., 335 (1988) 415; S.Turck-Chieze, talk given at the Intern. Conf. "Neutrino-92".
   I.-J.Sackmann et al., Astroph. J., 360 (1990) 727.
8. J.N.Bahcall and H.A.Bethe, Phys.Rev.Lett., 67 (1990) 2233.
   J.N.Bahcall, these Proceedings.
9. P.I.Krastev, S.P.Mikheyev and A.Yu.Smirnov, INR-preprint 0695 (1991).
10. J.M.Gelb, W.Kwong and S.P.Rosen, Phys.Rev.Lett., 69 (1992) 1864.
11. P.I.Krastev and S.T.Petcov, Preprint CERN-TH.6539/92 (to be published in Phys.Lett.B, (1992).
12. S.P.Mikheyev and A.Yu.Smirnov, in preparation.
13. P.Anselmann et al., Phys. Lett., B285 (1992) 389.
14. S.A.Bludman, N.Hata, D.C.Kennedy and P.G.Langacker, Preprint UPR-0516T (1992).
15. J.N.Bahcall and W.C.Haxton, Phys.Rev., D40 (1989) 931.
16. X.Shi, D.N.Schramm and J.N.Bahcall, Preprint 92-26-EFI-UofC (submitted to Phys.Rev.Lett.).
17. L.Krauss, E.Gates and M.White, Preprint YCTP-P38-92.
18. S.P.Mikheyev and A.Yu.Smirnov, Phys. Lett., B200 (1989) 560.
19. X.Shi and D.Schramm, Phys. Lett., B283 (1992) 305 .
20. M.Fukugita and Yanagida, Preprint PIFP-738.
21. M.M.Guzzo, A.Masiero and S.Petcov, Phys. Lett., B260 (1991) 154.
22. E.Roulet, Phys.Rev., D44 (1991) R935.
23. V.Barger, R.J.N.Phillips and K.Whisnant, Phys.Rev., D44 (1991) 1629.
24. P.Krastev, A.Masiero, S.Petcov and A.Yu.Smirnov in preparation (see A.Yu.Smirnov, Proc. of the 4th Int. Symp. on "Neutrino Telescopes" (1992)).